

Ayşe Betül ÖZTÜRK¹
Nurhan AKARAS²
Hasan ŞİMŞEK³
Fatih Mehmet KANDEMİR⁴



¹Department of Pediatric Surgery, Aksaray University, Faculty of Medicine, Aksaray, Türkiye.

²Department of Histology and Embryology, Aksaray University, Faculty of Medicine, Aksaray, Türkiye.

³Department of Physiology, Aksaray University, Faculty of Medicine, Aksaray, Türkiye.

⁴Department of Medical Biochemistry, Aksaray University, Faculty of Medicine, Aksaray, Türkiye.



Geliş Tarihi/Received :28.10.2024
Kabul Tarihi/Accepted :19.02.2025
Yayın Tarihi/Publication Date :17.03.2025

Sorumlu Yazar/Corresponding author:

Ayşe Betül Öztürk

E-mail: abetulozturk@aksaray.edu.tr

Cite this article: Öztürk, A., B., Akaras, N., Şimşek H., Kandemir, F. M. (2025).

Investigation of the Effects of Chrysin on Intestinal Ischemia-Reperfusion via Apoptotic, Oxidative Stress, Inflammation, and Autophagy Parameters. *Journal of Laboratory Animal Science and Practices*. 5(1), 49-59.

<https://doi.org/10.62425/jlasp.1574905>



Content of this journal is licensed under a Creative Commons Attribution-Noncommercial 4.0 International License.

Investigation of the Effects of Chrysin on Intestinal Ischemia-Reperfusion via Apoptotic, Oxidative Stress, Inflammation, and Autophagy Parameters

Chrysin'in Bağırsak İskemi-Reperfüzyonu Üzerindeki Etkilerinin Apoptotik, Oksidatif Stres, İnflamasyon ve Otofaji Parametreleri Aracılığıyla Araştırılması

ABSTRACT

This study aimed to investigate chrysin's molecular, biochemical, and histological effects in an experimental intestinal ischemia/reperfusion (IR) model and to reveal possible protective mechanisms. 35 Wistar rats were randomly divided into five groups: Control, CHR, IR, IR+CHR25, IR+CHR50. The IR model was established by inducing ischemia by ligating the superior mesenteric artery for one hour and restoring blood flow for two hours. In the study, MDA and GSH levels were analysed by manuel biochemical method; SOD, CAT, GPx activities and NF-κB and NO levels by ELISA method; caspase-3, Beclin-1, LC3A, PERK, ATF-6 mRNA transcription levels by RT-PCR method. In addition, tissue structure was examined histologically. MDA levels were doubled in the IR group and decreased with CHR ($p < .05$). In addition, CHR increased SOD, CAT and GPx activities and GSH levels which decreased due to IR ($p < .05$). Inflammation markers NF-κB and NO were increased; and decreased with CHR ($p < .05$). Apoptosis marker caspase-3 increased in IR and decreased with CHR ($p < .05$). Autophagy markers Beclin-1 and LC3A were increased by CHR ($p < .05$); endoplasmic reticulum stress markers PERK and ATF-6 were increased in IR and decreased by CHR ($p < .05$). Severe histopathologic changes were observed in the IR and improved with CHR treatment. While IR causes damage to intestinal tissue, the antioxidant and anti-inflammatory properties of CHR have revealed its therapeutic potential against IR injury.

Keywords: Apoptosis, Autophagy, Chrysin, Inflammation, Intestinal, Ischemia/reperfusion.

Öz

Bu çalışmanın amacı, deneysel bağırsak iskemi/reperfüzyon (IR) modelinde chrysin'in moleküler, biyokimyasal ve histolojik etkilerini araştırmak ve olası koruyucu mekanizmaları ortaya çıkarmaktır. 35 Wistar sıçan rastgele beş gruba ayrıldı: Kontrol, CHR, IR, IR+CHR25, IR+CHR50. IR modeli, superior mezenterik arterin bir saat süreyle bağlanmasıyla iskemi oluşturularak ve ardından iki saat süreyle kan akışının yeniden sağlanmasıyla oluşturulmuştur. Çalışmada manuel biyokimyasal yöntemle MDA ve GSH düzeyleri; ELISA yöntemiyle SOD, CAT, GPx aktiviteleri ile NF-κB, ve NO düzeyleri; RT-PCR yöntemiyle caspase-3, Beclin-1, LC3A, PERK, ATF-6 mRNA transkripsiyon düzeyleri analiz edildi. Ayrıca, histolojik olarak doku yapısı incelendi. MDA düzeyleri IR grubunda iki katına çıkarken, CHR ile azaldı ($p < .05$). Ayrıca CHR, IR'ye bağlı azalan SOD, CAT ve GPx aktiviteleri ile GSH düzeylerini arttırdı ($p < .05$). İnflamasyon belirteçleri NF-κB, ve NO artmış; CHR ile azalmıştır ($p < .05$). Apoptoz belirteçlerinden kaspaz-3 IR'de arttı ve CHR ile azaldı ($p < .05$). Otofaji belirteçleri Beclin-1 ve LC3A CHR ile arttı ($p < .05$); endoplazmik retikulum stresi belirteçleri PERK ve ATF-6 IR'de arttı ve CHR ile azaldı ($p < .05$). IR'de ciddi histopatolojik değişiklikler gözlemlendi ve CHR tedavisi ile düzeldi. IR, bağırsak dokusunda hasara yol açarken, CHR'nin antioksidan ve anti-inflamatuvar özellikleri, bağırsak IR hasarına karşı terapötik potansiyelini ortaya koymuştur.

Anahtar kelimeler: Apoptoz, Bağırsak, Chrysin, İnflamasyon, İskemi/reperfüzyon, Otofaji.

Introduction

The term ischemia is used to describe a reduction or cessation of blood flow to an organ due to obstructions or mechanical causes. The restoration of blood flow is referred to as reperfusion. Reperfusion plays a pivotal role in restoring normal function to ischemic tissue; however, it also precipitates reperfusion injury (Agartan et al., 2022). Intestinal ischemia-reperfusion (IR) injury affects patient outcomes and healthcare costs. The condition is caused by an obstruction of the superior mesenteric artery due to various underlying factors. This ultimately leads to significant damage to the affected tissue, which may be localized or extensive. Subsequently, the potential for the development of multiple organ failure exists. Intestinal ischemia may result from several intravascular pathologies, including arterial thrombosis, embolism, Henoch-Schönlein purpura, disseminated intravascular coagulation, or external compression of the vessels, such as volvulus, intussusception, strangulated inguinal hernia, tumor, or fibrotic band (Badak et al., 2014).

Chrysin (CHR) is a naturally occurring flavonoid with a 5,7-dihydroxyl structure. It is a naturally occurring substance found in honey, propolis, flowers, and mushrooms (Kandemir et al., 2017). CHR has been demonstrated to have no adverse effects. This substance has many pharmacological effects, including antioxidant, anti-inflammatory, anticancer, antiallergic, antiaging, antidiabetic, and antiapoptotic properties (Aksu et al., 2018). CHR is a benzene-heterocyclic hybrid. The molecule has two to three double-bonded carbons and a carbonyl group on the fourth. It is worthy of note that the three-carbon hydroxyl group is absent. Furthermore, the fifth and seventh carbon atoms exhibit the presence of hydroxyl functional groups (-OH). Unlike other flavonoids, CHR does not undergo oxygenation in Ring-B. The primary factor contributing to A-ring oxygenation diversity is responsible for various derivatives, including wogonin, baicalein, and oroxylin A. CHR's biological activities result from the absence of oxygenation in the B and C rings, which produce anti-inflammatory and antitoxic effects. The antioxidant activity of different flavones is also predicted to depend on their structure. The carbonyl group at C-4 and the double bond between C-2 and C-3 are associated with CHR's antioxidant activity (Talebi et al., 2021).

The objective of the present study was to examine the molecular, biochemical, and histological consequences of CHR on intestinal tissue in rats with experimental intestinal

IR, with the aim of elucidating potential mechanisms of action.

Methods

Ethical Approval

The ethics committee that approved the study was the Ethics Committee of Necmettin Erbakan University KONUDAM Experimental Medicine Application and Research Center (No: 2024/35, Date: 22.03.2024).

Experimental Design

A total of 35 *Wistar albino* rats, weighing between 220 and 250 grams and aged between 10 and 12 weeks, were utilized in the experiment. The animals were maintained in cages within a controlled environment with a constant temperature of 24-25°C and a twelve (12h) hour dark-light cycle (07:00-19:00 light; 19:00-07:00 dark). The subjects were provided with unlimited access to water and a standard diet. Following a one-week period during which the rats were permitted to acclimate to their surroundings, the experiments were initiated.

The rats were randomly assigned to one of five groups, with each group comprising seven rats.

Groups;

1: Control Group: For three days, the subjects received an oral administration of saline solution once per day.

2: Chrysin Group (CHR): A single daily oral administration of CHR at a dosage of 50 mg/kg was conducted over a three-day period.

3: Intestinal IR Group (IR): For a period of three days, the subjects received a single daily oral administration of saline solution. On day 4, the IR model was applied.

4: Intestinal IR Group +Chrysin-25 (IR+CHR25): A single daily oral administration of CHR at a dosage of 25 mg/kg was conducted over a three-day period. On day 4, the IR model was applied.

5: Intestinal IR Group +Chrysin-50 (IR+CHR50): The administration of CHR at a dosage of 50 mg/kg was conducted once daily via oral gavage for a period of three days. On day 4, the IR model was applied.

CHR (cas no: 480-40-0, purity 97%) was obtained from Sigma Chemical Co. (St. Louis, US). CHR doses were determined from the literature (Şimşek et al., 2023a). On the fourth day of the experiment, the IR model was applied.

Ischemia-reperfusion model

An intestinal IR model was constructed based on the methodology proposed by Li et al. (2022). Following laparotomy, the superior mesenteric artery (SMA) will be identified. An intestinal ischemia model was created by inducing ischemia for one hour. Following a period of one hour, the ligature was dislodged, and blood flow (reperfusion) was restored. The study was terminated two hours after the commencement of reperfusion.

Sampling

Immediately following the conclusion of the reperfusion period, the animals were euthanized via administration of ketamine-xylazine anesthesia, after which intestinal tissue (5 cm piece of jejunum) samples were obtained. Biochemical analyses were conducted on intestinal tissues, which were subsequently stored at -20°C until analysis. Intestinal tissues were pulverised to a diameter of 5 microns by grinding at 30.0 frequency 1/s for 30 seconds in a Qiagen TissueLyser II device with liquid nitrogen support. From the pulverised tissues, 50 mg samples were weighed and diluted to appropriate dilution coefficients with 1.15% KCl for malondialdehyde (MDA) and glutathione (GSH) analyses and PBS (pH 7.4) for ELISA analysis and homogenisation was performed using TissueLyser II. After centrifugation of the homogenates, supernatants were obtained by processing at 3,500 rpm for 15 minutes for MDA analysis, 11,000 rpm for 20 minutes for GSH analysis and 3,500 rpm for 20 minutes for ELISA.

Lipid peroxidation analysis

The level of lipid peroxidation was determined by measuring the absorbance at a wavelength of 532 nm of the color produced by the reaction of MDA and thiobarbituric acid in intestinal tissues. The method developed by Placer et al. (1966) was employed for the determination of MDA levels.

Antioxidant analysis

The antioxidant status of intestinal tissues was evaluated through the analysis of superoxide dismutase (SOD), catalase (CAT), and glutathione peroxidase (GPx) activities, employing commercial ELISA kits (Sunred, Shanghai, China, SOD:201-11-0169; CAT:201-11-5106; GPx:201-11-1705). The levels of GSH were quantified by the methodology proposed by Sedlak and Lindsay (1968). The total protein content of intestinal tissues was determined using the method of Lowry et al. (1951), which was also employed to calculate enzyme activities.

Inflammation Analysis

Nuclear Factor Kappa B (NF-κB), and Nitric Oxide (NO) elisa

kits (Sunred, Shanghai, China, NF-κB:201-11-5141; NO:201-11-0704) were measured according to the manufacturer's protocol.

Real Time PCR (RT-PCR)

The impact of IR injury and CHR treatment on the relative mRNA transcript levels of the gene regions enumerated in Table 1 in intestinal tissues obtained after the experiment was investigated through the use of the quantitative real-time polymerase chain reaction (qRT-PCR) method. Total RNA was isolated from tissues (100 mg) using the 1ml QIAzol Lysis Reagent (79306; Qiagen) kit. The cDNA synthesis was conducted using the OneScript Plus cDNA Synthesis Kit (ABM, G236, Richmond, Canada) for the synthesis of cDNA from isolated total RNA. The cDNA preparations were combined and subjected to a polymerase chain reaction (PCR) with primer sequences and BlasTaq™ 2X qPCR MasterMix (ABM, G891, Richmond, Canada). The reaction was conducted in a Rotor-Gene Q (Qiagen) apparatus, with the time and temperature cycles determined by the manufacturer's instructions. Once the cycles were complete, gene expression was normalized according to β-actin and evaluated using the 2-ΔΔCT method (Livak and Schmittgen, 2001).

Table 1. Primer sequences

Tablo 1. Primer dizilimleri

Gene	Sequences (5'-3')	Length (bp)	Accession No
Caspase-3	F: ACTGGAATGTCAGCTCGCAA R: GCAGTAGTCGCTCTGAAGA	270	NM_012922.2
PERK	F: GATGCCGAGAATCATGGGAA R: AGATTCGAGAAGGGACTCCA	198	NM_031599.2
ATF-6	F: TCAACTCAGCACGTTCTCTGA R: GACCAGTGACAGGCTTCTCT	130	NM_001107196.1
Beclin-1	F: TCTCGTCAAGGCGTCACTTC R: CCATTCTTTAGGCCCGACG	198	NM_053739.2
LC3A	F: GACCATGTAAACATGAGCGA R: CCTGTTTCATAGATGTCAGCG	139	NM_199500.2
β-Actin	F: CAGCCTTCCTTCTGGGTATG R: AGCTCAGTAACAGTCCGCCT	360	NM_031144.3

bp: base pair, Caspase-3: cysteine-aspartic acid protease 3, PERK: protein kinase R (PKR)-like endoplasmic reticulum kinase, ATF6: activating transcription factor 6, LC3A: microtubule-associated protein 1 light chain 3 alpha, β-Actin: beta actin

Histopathologic Method

Following the administration of IR and the agent, the intestinal tissues of the euthanized rats were excised and

washed with physiological serum. Subsequently, the tissues were preserved in a 10% formalin solution for 48 hours to facilitate fixation. Following the completion of the routine histologic follow-up, the tissues were embedded in paraffin, and 5- μ m-thick sections were subsequently prepared. The sections were stained with hematoxylin and eosin, and the stained tissues were evaluated and photographed using a light microscope (Olympus Cx43; Japan). The preparations were evaluated under light microscopy by a histologist in a blinded fashion according to the mesenteric IR injury scoring system described by Chiu et al. (1970). The lesions were evaluated and assigned a grade between 0 and 5 points. (0: normal mucosal villi, 1: subepithelial separations at the upper end of the villi with capillary congestion, 2: moderate intensity of subepithelial separations pushing the mucosal epithelium upward, 3: Subepithelial detachments with a substantial quantity of subepithelial detachments and deformations at the extremities of the villi, where the mucosal epithelium is subjected to considerable upward pressure along the villi. 4: Villus deformation with dilated capillaries reaching the lamina propria.

Statistical Analysis

The statistical analysis of the data obtained from the study was conducted using the IBM SPSS software (version 20.0; IBM Corp., North Castle, NY). The Shapiro-Wilk test was used to analyze the sample size, which was less than 50. Since the data had a normal distribution and there were more than two groups, Tukey's multiple comparison test and one-way analysis of variance (ANOVA) were used to compare differences between groups. The results were presented as mean \pm SE, with $p < .05$ considered to be statistically significant.

Results

Assessment of oxidant/antioxidant status

While MDA levels were employed to assess the oxidant status of intestinal tissue, SOD, CAT, and GPx activities and GSH levels were utilized to ascertain the antioxidant status (Figure 1, Table 2). The data indicated that MDA levels in the intestines of rats subjected to IR injury exhibited a twofold increase compared to the control and CHR groups ($p < .001$). The administration of CHR25 and CHR50 in conjunction with IR effectively suppressed lipid

peroxidation and reduced MDA levels ($p < .05$). Furthermore, the activities of SOD, CAT, and GPx, as well as the levels of GSH, were found to be diminished in the IR group when compared to the control and CHR groups ($p < .001$). However, the administration of both doses of CHR in conjunction with IR resulted in an enhancement of these activities and a reinforcement of the antioxidant system ($p < .05$). Additionally, it was determined that CHR demonstrated a dose-dependent effect, with the CHR50 dose exhibiting greater efficacy ($p < .05$).

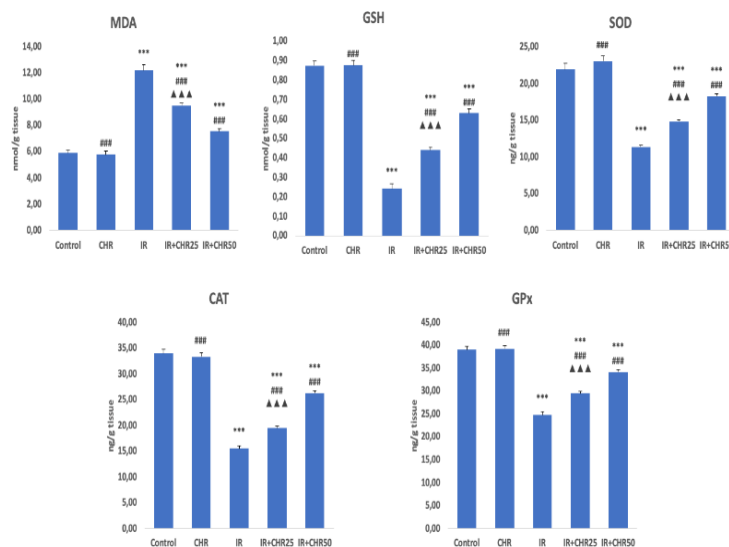


Figure 1. Intestinal tissue MDA and GSH levels and SOD, CAT, GPx activities after IR and CHR applications to rats. Statistical significance; MDA: malondialdehyde, GSH: Glutathione, SOD: superoxide dismutase, CAT: catalase, GPx: glutathione peroxidase, IR: ischemia reperfusion, CHR: Chrysin. Control and others: * $p < .05$, ** $p < .01$, *** $p < .001$, IR and others: # $p < .05$, ## $p < .01$, ### $p < .001$, IR + CHR25 and IR + CHR50: ▲ $p < .05$, ▲▲ $p < .01$, ▲▲▲ $p < .001$.

Şekil 1. Sıçanlara IR ve CHR uygulamalarından sonra bağırsak dokusu MDA ve GSH seviyeleri ve SOD, CAT, GPx aktiviteleri. İstatistiksel anlamlılık; MDA: malondealdehit, GSH: glutatyon, SOD: süperoksit dismutaz, CAT: katalaz, GPx: glutatyon peroksidaz, IR: iskemi reperfüzyon, CHR: Chrysin. Kontrol ve diğerleri: * $p < .05$, ** $p < .01$, *** $p < .001$, IR ve diğerleri: # $p < .05$, ## $p < .01$, ### $p < .001$, IR + CHR25 ve IR + CHR50: ▲ $p < .05$, ▲▲ $p < .01$, ▲▲▲ $p < .001$.

Table 2. Intestinal tissue oxidant and antioxidants activities after IR and CHR applications to rats

Tablo 2. Sıçanlara IR ve CHR uygulamaları sonrası bağırsak dokusu oksidan ve antioksidan aktiviteleri

	MDA	GSH	SOD	CAT	GPx
CONTROL	5.90±0.20 ^a	0.87±0.02 ^d	21.87±0.92 ^d	33.99±0.75 ^d	39.02±0.75 ^d
CHR	5.78±0.23 ^a	0.87±0.02 ^d	23.03±0.71 ^d	33.37±0.75 ^d	39.26±0.66 ^d
IR	12.21±0.44 ^d	0.24±0.02 ^a	11.37±0.24 ^a	15.55±0.53 ^a	24.77±0.75 ^a
IR+CHR25	9.51±0.15 ^c	0.44±0.01 ^b	14.81±0.24 ^b	19.44±0.41 ^b	29.51±0.41 ^b
IR+CHR50	7.56±0.17 ^b	0.63±0.02 ^c	18.30±0.32 ^c	26.33±0.45 ^c	34.20±0.43 ^c

MDA: malondialdehyde, GSH: Glutathione, SOD: superoxide dismutase, CAT: catalase, GPx: glutathione peroxidase, IR: ischemia reperfusion, CHR: chrysin. Different letters indicate statistical difference: * $p < .05$.

Markers of Inflammation

The levels of NF- κ B, and NO, which are markers of inflammation, were analyzed by ELISA kits (Figure 2, Table 3). The results demonstrated that there was no statistically significant difference between the control and CHR groups ($p > .05$). However, the intestinal levels of NF- κ B and NO in rats subjected to IR increased approximately twofold compared to the control and CHR groups. Additionally, the inflammation in this group was accelerated ($p < .001$). The combination of CHR doses with IR resulted in a notable reduction in NF- κ B, and NO levels, indicating an anti-inflammatory effect ($p < .05$). Notably, the inflammation levels were found to be elevated in rats subjected to IR ($p < .001$). The administration of both doses of CHR in conjunction with IR was observed to effectively suppress the inflammatory response ($p < .05$).

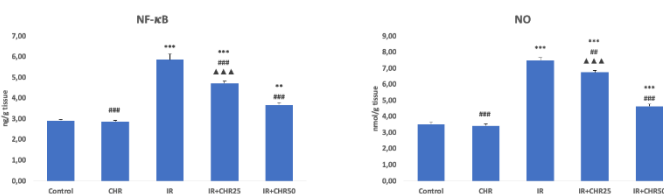


Figure 2: Intestinal tissue NF- κ B, and NO levels after IR and CHR applications to rats. Statistical significance; NF- κ B: nuclear factor kappa B, NO: nitric oxide, IR: ischemia reperfusion, CHR: Chrysin. Control and others: * $p < .05$, ** $p < .01$, *** $p < .001$, IR and others: # $p < .05$, ## $p < .01$, ### $p < .001$, IR + CHR25 and IR + CHR50: ▲ $p < .05$, ▲▲ $p < .01$, ▲▲▲ $p < .001$.

▲▲▲ $p < .001$.

Şekil 2. Sıçanlara IR ve CHR uygulamalarından sonra bağırsak dokusu NF- κ B ve NO seviyeleri. İstatistiksel anlamlılık; NF- κ B: nükleer faktör kappa B, NO: nitrik oksit, IR: iskemi reperfüzyon, CHR: Chrysin. Kontrol ve diğerleri: * $p < .05$, ** $p < .01$, *** $p < .001$, IR ve diğerleri: # $p < .05$, ## $p < .01$, ### $p < .001$, IR + CHR25 ve IR + CHR50: ▲ $p < .05$, ▲▲ $p < .01$, ▲▲▲ $p < .001$.

Apoptosis markers

mRNA transcription levels of cysteine aspartate-specific protease-3 (caspase-3), a key apoptotic marker, was evaluated through RT-PCR to ascertain the apoptotic status of intestinal tissues in rats subjected to experimental IR (Figure 3, Table 3). The data indicated that caspase-3 levels were elevated in IR-treated rat intestinal tissues relative to the control and CHR groups, resulting in accelerated apoptosis ($p < .001$). The combination of CHR25 and CHR50 doses with IR resulted in a reduction in caspase-3 levels compared to the IR group, indicating an antiapoptotic effect through the suppression of apoptosis ($p < .05$).

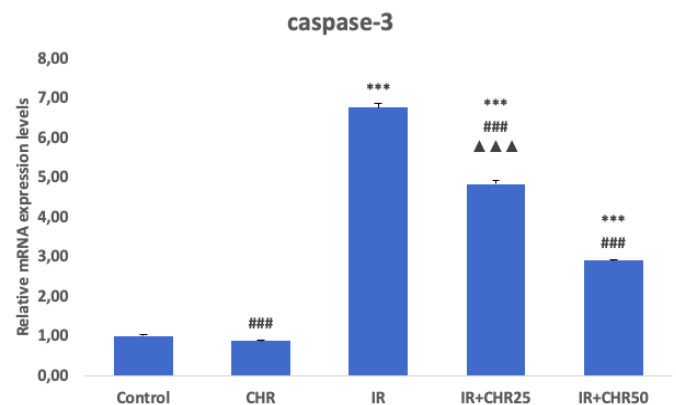


Figure 3: Intestinal tissue caspase-3 mRNA transcription levels after IR and CHR applications to rats. Caspase-3: cysteine-aspartic acid protease 3, IR: ischemia reperfusion, CHR: Chrysin. Statistical significance; Control and others: * $p < .05$, ** $p < .01$, *** $p < .001$, IR and others: # $p < .05$, ## $p < .01$, ### $p < .001$, IR + CHR25 and IR + CHR50: ▲ $p < .05$, ▲▲ $p < .01$, ▲▲▲ $p < .001$.

Şekil 3. Sıçanlara IR ve CHR uygulamaları sonrası bağırsak dokusu kaspaz-3 mRNA transkripsiyon seviyeleri. Kaspaz-3: sistein-aspartik asit proteaz 3, IR: iskemi reperfüzyon, CHR: Chrysin. İstatistiksel anlamlılık; Kontrol ve diğerleri: * $p < .05$, ** $p < .01$, *** $p < .001$, IR ve diğerleri: # $p < .05$, ## $p < .01$, ### $p < .001$, IR + CHR25 ve IR + CHR50: ▲ $p < .05$, ▲▲ $p < .01$, ▲▲▲ $p < .001$.

Table 3. Intestinal tissue NF- κ B, NO levels and caspase-3 mRNA transcription levels after IR and CHR applications to rats

Tablo 3. Sıçanlara IR ve CHR uygulamalarından sonra bağırsak dokusu NF- κ B, NO seviyeleri ve kaspaz-3 mRNA transkripsiyon seviyeleri

	NF- κ B	NO	caspase-3
CONTROL	2.92 \pm 0.07 ^a	3.53 \pm 0.11 ^a	1.00 \pm 0.05 ^a
CHR	2.87 \pm 0.06 ^a	3.43 \pm 0.11 ^a	0.87 \pm 0.03 ^a
IR	5.87 \pm 0.26 ^d	7.49 \pm 0.16 ^d	6.77 \pm 0.09 ^d
IR+CHR25	4.72 \pm 0.10 ^c	6.75 \pm 0.11 ^c	4.84 \pm 0.08 ^c
IR+CHR50	3.68 \pm 0.09 ^b	4.65 \pm 0.12 ^b	2.92 \pm 0.01 ^b

NF- κ B: Nuclear factor kappa B, NO: nitric oxide, caspase-3: cysteine aspartate-specific protease-3, IR: ischemia reperfusion, CHR: Chrysin. Different letters indicate statistical difference: * p < .05.

Effect of CHR on mRNA transcription levels of autophagic gene

mRNA transcription levels of Beclin-1, microtubule-associated protein 1 light chain 3 alpha (LC3A) were analyzed for determining autophagic damage (Figure 4, Table 4). The result of the analysis revealed that autophagic damage led to an increase in the levels of Beclin-1 and L3CA in the CHR-treated group compared to the control (p < .001). Autophagic damage was reduced in the CHR50 treated group with lower levels of Beclin-1 (p < .001) and L3CA (p < .001) compared to the CHR25 treated group.

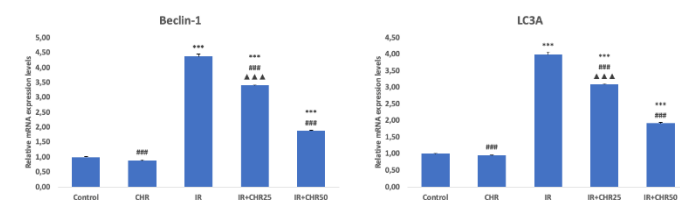


Figure 4: Intestinal tissue Beclin-1, and LC3A mRNA transcription levels after IR and CHR applications to rats. LC3A: microtubule-associated protein 1 light chain 3 alpha, IR: ischemia reperfusion, CHR: Chrysin. Statistical significance; Control and others: * p < .05, ** p < .01, *** p < .001, IR and others: # p < .05, ## p < .01, ### p < .001, IR + CHR25 and IR + CHR50: Δ p < .05, $\Delta\Delta$ p < .01, $\Delta\Delta\Delta$ p < .001.

Şekil 4: Sıçanlara IR ve CHR uygulamalarından sonra bağırsak dokusu Beclin-1 ve LC3A mRNA transkripsiyon

seviyeleri. LC3A: mikrotübül ilişkili protein 1 hafif zincir 3 alfa, IR: iskemi reperfüzyonu, CHR: Chrysin. İstatistiksel anlamlılık; Kontrol ve diğerleri: * p < .05, ** p < .01, *** p < .001, IR ve diğerleri: # p < .05, ## p < .01, ### p < .001, IR + CHR25 ve IR + CHR50: Δ p < .05, $\Delta\Delta$ p < .01, $\Delta\Delta\Delta$ p < .001.

Effects of CHR on endoplasmic reticulum stress markers in intestinal tissue

Endoplasmic reticulum (ER) stress in intestinal tissue was evaluated by analysis of expression levels of activating transcription factor 6 (ATF-6), and protein kinase R-like endoplasmic reticulum kinase (PERK) genes (Figure 5, Table 4). IR caused ER stress in intestinal tissue and induced the expression of related genes (p < .001). On the other hand, CHR treatment suppressed ER stress and decreased the relative mRNA transcript levels of ATF-6, and PERK (p < .001). When the doses were compared in the study, it was determined that CHR50 was more effective on ATF-6 (p < .001) and PERK (p < .01) genes than CHR25.

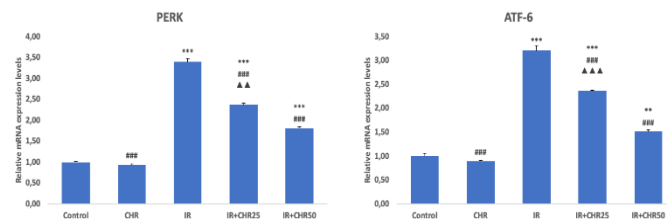


Figure 5: Intestinal tissue PERK, and ATF-6 mRNA transcription levels after IR and CHR applications to rats. PERK: protein kinase R (PKR)-like endoplasmic reticulum kinase, ATF6: activating transcription factor 6, IR: ischemia reperfusion, CHR: Chrysin. Statistical significance; Control and others: * p < .05, ** p < .01, *** p < .001, IR and others: # p < .05, ## p < .01, ### p < .001, IR + CHR25 and IR + CHR50: Δ p < .05, $\Delta\Delta$ p < .01, $\Delta\Delta\Delta$ p < .001.

Şekil 5: Sıçanlara IR ve CHR uygulamalarından sonra bağırsak dokusu PERK ve ATF-6 mRNA transkripsiyon seviyeleri. PERK: protein kinaz R (PKR) benzeri endoplazmik retikulum kinaz, ATF6: aktive edici transkripsiyon faktörü 6, IR: iskemi reperfüzyon, CHR: Chrysin. İstatistiksel anlamlılık; Kontrol ve diğerleri: * p < .05, ** p < .01, *** p < .001, IR ve diğerleri: # p < .05, ## p < .01, ### p < .001, IR + CHR25 ve IR + CHR50: Δ p < .05, $\Delta\Delta$ p < .01, $\Delta\Delta\Delta$ p < .001.

Table 4. Intestinal tissue ER stress and autophagy parameters levels after IR and CHR applications to rats

Tablo 4. Sıçanlara IR ve CHR uygulamalarından sonra bağırsak dokusu ER stresi ve otofaji parametreleri düzeyleri

	PERK	ATF-6	Beclin-1	LC3A
CONTROL	1.00±0.02 ^a	1.00±0.06 ^a	1.00±0.02 ^a	1.00±0.02 ^a
CHR	0.93±0.03 ^a	0.89±0.01 ^a	0.88±0.03 ^a	0.95±0.02 ^a
IR	3.40±0.08 ^d	3.21±0.11 ^d	4.37±0.07 ^d	4.00±0.07 ^d
IR+CHR25	2.37±0.04 ^c	2.37±0.01 ^c	3.41±0.01 ^c	3.09±0.03 ^c
IR+CHR50	1.81±0.03 ^b	1.52±0.03 ^b	1.88±0.01 ^b	1.92±0.02 ^b

Beclin-1, microtubule-associated protein 1 light chain 3 alpha (LC3A), activating transcription factor 6 (ATF-6), and protein kinase R-like endoplasmic reticulum kinase (PERK), IR: ischemia reperfusion, CHR: chrysin. Different letters indicate statistical difference: * $p < .05$.

Histopathologic Results

The intestinal light microscopic structures of the experimental groups are illustrated in Figure 6. Upon examination of the intestinal tissues of the control and CHR groups, it was observed that the mucosa, submucosa, muscularis, and adventitia layers exhibited a normal histologic structure. The mucosa exhibited the presence of normally organized villi, goblet cells, and enterocyte cells (Figure 6A, 6B). In comparison to the control group, rats that underwent IR exhibited a multitude of pathological alterations. These included severe epithelial shedding, mucosal edema, degeneration and necrotic changes in epithelial cells, disruption of villi, inflammatory cell infiltration, vascular congestion and hemorrhage (Figure 6C). However, in the IR+CHR groups, the mucosa exhibited partial healing and was comparable to the control group. At a lower level, there was evidence of villus disruption, congestion, and inflammatory cell infiltration (Figure 6D, 6E). The Chiu score of the intestinal mucosa was observed to be higher in the IR group than in the control group. Although the mean scores of the groups administered CHR with IR application were higher than those of the control group, they were lower than those of the other groups due to the healing of the intestinal mucosa layers. A statistically significant difference was observed between the groups with regard to the histopathologically determined chiu damage scores (Figure 6F).

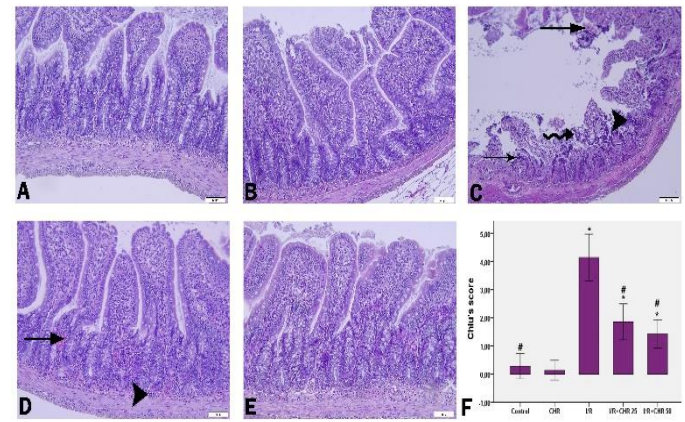


Figure 6. Representative micrographs of the effects of CHR on the microscopic structure of intestinal tissue following IR injury (H&E staining, bar = 50 μ m). The normal histologic structure of the mucosa, submucosa, muscularis, and adventitia of the control (A) and CHR (B) groups is presented. In the intestinal villi, IR (C) resulted in disorganization, and exfoliation of epithelial cells (curved arrow), as well as degeneration and necrotic changes in epithelial cells (thin arrow). Additionally, severe mononuclear cellular infiltration (arrowhead) was observed. In IR+CHR25 (D) and IR+CHR50 (E), mild mononuclear cellular infiltration (arrowhead) and mild vascular congestion and hemorrhage (thick arrow) were evident. The Chi-square score (F) for the various groups was found to be statistically significant ($p < .05$) when compared to the control group, and also when compared to the IR group ($p < .05$).

Şekil 6. IR hasarını takiben CHR'in bağırsak dokusunun mikroskopik yapısı üzerindeki etkilerinin temsili mikroyrafları (H&E boyama, bar = 50 μ m). Kontrol (A) ve CHR (B) gruplarının mukoza, submukoza, muskularis ve adventisyanın normal histolojik yapısı sunulmuştur. Bağırsak villuslarında, IR (C) intestinal villuslar düzensiz ve epitel hücrelerinin eksfoliasyonu (kıvrık ok) yanı sıra epitel hücrelerinde dejenerasyon ve nekrotik değişikliklerle (ince ok) sonuçlanmıştır. Ek olarak, şiddetli mononükleer hücre infiltrasyonu (ok başı) gözlenmiştir. IR+CHR25 (D) ve IR+CHR50'de (E), hafif mononükleer hücre infiltrasyonu (ok başı) ve hafif vasküler konjesyon ve hemoraji (kalın ok) belirlendi. Çeşitli gruplar için Ki-kare skoru (F) kontrol grubuyla karşılaştırıldığında ($p < .05$) ve IR grubuyla karşılaştırıldığında ($p < .05$) istatistiksel olarak anlamlı bulunmuştur.

Discussion

Acute intestinal ischemia represents one of the most prevalent forms of intestinal ischemia and is a significant circulatory disorder of the gastrointestinal tract. It is an important clinical entity with a high morbidity and mortality rate. The duration of ischemia has a direct impact on the prognosis of the patient, underscoring the vital importance of early diagnosis and treatment. Conversely, reperfusion and ischemia have been demonstrated to contribute to the damage (Kuzu et al., 1998).

In a study conducted by Park et al. (1992), no mucosal damage was observed in rats exposed to 20 minutes of strangulation ischemia. However, when the ischemia was prolonged to over 20 minutes, villus damage was evident. Furthermore, when the strangulation exceeded 60 minutes, transmucosal damage occurred. In a subset of the study, 8-12 hours of total or near-total ischemia resulted in transmural gangrene. The authors assert that there is no evidence to suggest that reperfusion exacerbates ischemic damage in instances of ischemia lasting less than 20 minutes or exceeding 8-12 hours. Additionally, they propose that the most significant damage occurs when IR persists for 40-60 minutes (Park et al., 1992). In contrast, Megison et al. (1990) reported a mortality rate of 70% in a 30-minute deep intestinal ischemia model, which is considered a reproducible and reliable model in the literature.

The lack of reduction in the mortality and morbidity rates associated with mesenteric ischemia, coupled with the challenges encountered in its clinical management, has prompted us to undertake a comprehensive investigation into this area. To this end, we constructed an experimental intestinal IR model in rats and investigated the impact of CHR. The objective of our study was to demonstrate the potential protective effect of CHR in intestinal IR injury. Ischemia is the death of cells caused by inadequate blood flow, low energy, and toxic build-up. Ischemic tissues require restoration of blood flow in order to facilitate cell regeneration and the elimination of toxic metabolites. However, reperfusion has the opposite effect, causing damage to the tissue that is much more severe than that caused by the ischemic process. The damage caused by reperfusion can be attributed to a number of factors, the majority of which are oxygen-derived free radicals (Ali et al., 2019). Reactive oxygen species (ROS) damage DNA, cell membranes, and mitochondria through processes like lipid peroxidation and cytokine production from activated neutrophils (Akaras et al., 2023a). Free radicals, oxidative stress, and inflammation are thought to be the main causes

of intestinal IR injury (Ali et al., 2019). The present study demonstrated that MDA levels, the end product of lipid peroxidation, were elevated in rat intestinal tissues subjected to IR injury. Concurrently, reduced GSH levels and SOD, CAT, and GPx activities, which are integral components of the antioxidant defense system, exhibited a decline. Consequently, oxidative stress was observed to increase. The administration of CHR was observed to be efficacious in safeguarding the intestines from oxidative damage induced by IR, as evidenced by a reduction in MDA levels and an augmentation in GSH, SOD, CAT, and GPx activities. The study conducted by Güvenç et al. (2024) demonstrated that intestinal IR increased MDA levels, decreased antioxidant activities such as GSH, CAT, and GPx, and caused the development of oxidative stress. The application of flavonoids was found to be an effective method of protecting tissues from IR damage.

NOS synthesizes NO. In the rat intestine, the dominant enzymes are endothelial NOS (eNOS) and inducible NOS (iNOS). An excess of intracellular NO causes cell death by generating ROS and peroxynitrite (Refaie and El-Hussieny, 2018). The present study demonstrated that intestinal NO levels increased in IR-induced rats, and that both doses of CHR administration were effective in protecting the intestines from IR-induced nitrosative stress by decreasing NO levels. Intestinal IR injury occurs through an inflammatory response, which plays a pivotal role in its pathogenesis. Oxidative stress releases proinflammatory cytokines (İleriturk et al., 2024). NF- κ B is a master regulatory transcription factor that regulates inflammatory responses and co-localizes with I κ B in the cytoplasm. Upon phosphorylation by protein kinases, I κ B is released, allowing NF- κ B to enter the nucleus and regulate proinflammatory cytokines, including TNF- α and IL-1 β (Yesildag et al., 2022). The present study demonstrated that NF- κ B levels were elevated and that intestinal inflammation was enhanced in IR-induced intestines. These observations suggest that oxidative stress may have been a contributing factor in the observed increase. Zou et al. (2003) found that IR injury in the intestine elevates proinflammatory cytokines and cellular inflammation. A number of studies have demonstrated that flavonoids possess anti-inflammatory properties, which are mediated by the suppression of NF- κ B expression (Kandemir et al., 2022; Kankılıç et al., 2024).

Apoptosis is a programmed cell death that eliminates damaged cells (Simsek and Akaras, 2023). Nevertheless, excessive apoptosis has been demonstrated to result in damage to a range of tissues (Yıldız et al., 2022). The caspase family of proteins plays a pivotal role in the

regulation of apoptosis (Akaras et al., 2023b). It is well established that oxidative stress plays a regulatory role in apoptosis through its interaction with caspase family proteins. Caspase-3 is a crucial indicator of apoptosis, and its activation is contingent upon caspase-9 activation (Semis et al., 2021). It has been demonstrated that intestinal IR elevates caspase-3 levels and triggers apoptosis (Afolabi et al., 2022; Osmanlioğlu et al., 2023). Similarly, the present study demonstrated that caspase-3 expression increased in intestinal tissue subjected to IR, and the apoptotic process accelerated with the concomitant increase in oxidative stress and inflammation. However, the combination of CHR with IR proved effective in suppressing oxidative stress and inflammation, as well as protecting the cell from apoptosis by decreasing caspase-3 expression. The literature indicates that CHR exerts an antiapoptotic effect by inhibiting caspase-3 (Yardımcı et al., 2021; Yakut et al., 2024).

The ER fulfills a multitude of functions, including the maintenance of cellular homeostasis, the detoxification of xenobiotics, and the regulation of calcium homeostasis. Conversely, the disequilibrium that arises in a multitude of physiological and pathological processes gives rise to ER stress, whereby the aggregation of unfolded or misfolded proteins within the ER lumen ensues (Rana et al., 2020; İlleritürk et al., 2023). The unfolded protein response (UPR) is activated in response to ER stress to maintain protein homeostasis. The UPR response is characterised by the presence of three distinct effectors. The aforementioned proteins are ATF-6, and PERK (Şimşek et al., 2023b). Nevertheless, the continuity of the UPR has deleterious consequences, including apoptosis (Celik et al., 2020). It has been previously demonstrated that IR results in an elevation of ER stress markers in tissues (Zhou et al., 2018). Similarly, our study demonstrated that following CHR application, ATF-6 and PERK expressions were triggered. Given the link between ER stress and oxidative stress, we postulated that CHR could combat ER stress. CHR treatment reduced mRNA levels of ATF-6 and PERK in intestinal tissue, indicating a potential beneficial effect on intestinal tissue.

The essential proteins involved in autophagy are Beclin-1 and LC3A (Şimşek et al., 2023c). Beclin-1 is linked to tumor suppression and immune function. This protein forms the phosphoinositide 3-kinase (PI3K) complex (He et al., 2010). Beclin-1 and LC3A are autophagic markers that demonstrate increased expression during reperfusion. The present study demonstrated that CHR was associated with

a reduction in the levels of Beclin-1 and LC3A.

Conclusion

Upon evaluation of the data obtained from the study, it was determined that IR caused tissue damage while inducing oxidative stress, inflammation, and apoptosis in intestinal tissue. CHR demonstrated antioxidant, anti-inflammatory, and anti-apoptotic effects, as well as promoting cell proliferation. Consequently, its use in intestinal IR was determined to be beneficial.

Ethics Committee Approval: The ethics committee that approved the study was the Ethics Committee of Necmettin Erbakan University KONUDAM Experimental Medicine Application and Research Center (No: 2024/35, Date: 22.03.2024).

Author Contributions: Concept – ABÖ, FMK; Design – ABÖ, FMK; Supervision – FMK; Resources – ABÖ; Materials – ABÖ, NA, HŞ, FMK; Data Collection and/or Processing – ABÖ, NA, HŞ, FMK; Analysis and/or Interpretation – ABÖ, NA, HŞ, FMK; Literature Search – ABÖ; Writing Manuscript – ABÖ; Critical Review – ABÖ, HŞ, FMK

Peer-review: Externally peer-reviewed.

Funding: This study was not funded by any institution.

Declaration of Interests: The authors declare that they have no competing interest.

References

- Afolabi, O. A., Hamed, M. A., Anyogu, D. C., Adeyemi, D. H., Odetayo, A. F., & Akhigbe, R. E. (2022). Atorvastatin-mediated downregulation of VCAM-1 and XO/UA/caspase 3 signaling averts oxidative damage and apoptosis induced by ovarian ischaemia/reperfusion injury. *Redox report*, 27(1), 212-220. <https://doi.org/10.1080/13510002.2022.2129192>
- Agartan, E. S., Mogulkoc, R., Baltaci, A. K., Menevse, E., Dasdelen, D., & Avunduk, M. C. (2022). 3', 4'-Dihydroxyflavonol (DiOHF) prevents DNA damage, lipid peroxidation and inflammation in ovarian ischaemia-reperfusion injury of rats. *Journal of obstetrics and gynaecology*, 42(2), 338-345. <https://doi.org/10.1080/01443615.2021.1916813>
- Akaras, N., Kandemir, F. M., Şimşek, H., Gür, C., & Aygörmec, S. (2023a). Antioxidant, Antiinflammatory, and Antiapoptotic Effects of Rutin in Spleen Toxicity Induced by Sodium Valproate in Rats. *Türk doğa ve fen dergisi*, 12(2), 138-144. <https://doi.org/10.46810/tdfd.1299663>
- Akaras, N., Gür, C., Şimşek, H., & Tuncer, S. Ç. (2023b). Effects of Quercetin on Cypermethrin-Induced Stomach Injury: The Role of Oxidative Stress, Inflammation, and Apoptosis. *Gümüşhane üniversitesi sağlık bilimleri dergisi*, 12(2), 556-566. <https://doi.org/10.37989/gumussagbil.1225539>
- Aksu, E. H., Kandemir, F. M., Küçükler, S., & Mahamadu, A. (2018). Improvement in colistin-induced reproductive damage, apoptosis, and autophagy in testes via reducing oxidative stress by chrysin. *Journal of biochemical and molecular toxicology*, 32(11), e22201. <https://doi.org/10.1002/jbt.22201>

- Ali, F. F., Ahmed, A. F., & Ali, D. M. E. (2019). Underlying mechanisms behind the protective effect of angiotensin (1–7) in experimental rat model of ovarian ischemia reperfusion injury. *Life sciences*, 235, 116840. <https://doi.org/10.1016/j.lfs.2019.116840>
- Aydın, G., Gökçimen, A., Öncü, M., Çicek, E., Karahan, N., & Gökalp, O. (2003). Histopathologic changes in liver and renal tissues induced by different doses of diclofenac sodium in rats. *Turkish journal of veterinary & animal sciences*, 27(5), 1131-1140.
- Badak B, Turk O, Caga T, Burukoglu D. (2014). The protective effect of milrinone on ischemia/reperfusion injury on superior mesenteric artery ligated rats. *Journal of surgical arts* 7 (1), 1-6.
- Brandt, L. J., & Boley, S. J. (1993). Ischemic and vascular lesions of the bowel. In M. H. Sleisenger & J. S. Fordtran (Eds.), *Gastrointestinal disease* (5th ed., pp. 1822–1844). W.B. Saunders.
- Celik H, Kucukler S, Ozdemir S, Comakli S, Gur C, Kandemir FM, et al. (2020). Lycopene protects against central and peripheral neuropathy by inhibiting oxaliplatin-induced ATF-6 pathway, apoptosis, inflammation and oxidative stress in brains and sciatic tissues of rats. *Neurotoxicology*. 80:29-40. <https://doi.org/10.1016/j.neuro.2020.06.005>
- Chiu, C. J., McArdle, A. H., Brown, R., Scott, H. J., & Gurd, F. N. (1970). Intestinal mucosal lesion in low-flow states: I. A morphological, hemodynamic, and metabolic reappraisal. *Archives of surgery*, 101(4), 478-483. <https://doi.org/10.1001/archsurg.1970.01340280030009>
- Grace, P. (1994). Ischemia-reperfusion injury/PA Grace. *British journal of surgery*, 81(5), 637-647. <https://doi.org/10.1002/bjs.1800810504>
- Güvenç, M., Yüksel, M., Kutlu, T., Etyemez, M., Gökçek, İ., & Cellat, M. (2024). Protective effects of esculetin against ovary ischemia–reperfusion injury model in rats. *Journal of biochemical and molecular toxicology*, 38(1), e23528. <https://doi.org/10.1002/jbt.23528>
- He, C., & Levine, B. (2010). The beclin 1 interactome. *Current opinion in cell biology*, 22, 140–149. <https://doi.org/10.1016/j.ceb.2010.01.001>
- Ileriturk, M., Ileriturk, D., Kandemir, O., Akaras, N., Simsek, H., Erdogan, E., & Kandemir, F. M. (2024). Naringin attenuates oxaliplatin-induced nephrotoxicity and hepatotoxicity: A molecular, biochemical, and histopathological approach in a rat model. *Journal of biochemical and molecular toxicology*, 38(1), e23604. <https://doi.org/10.1002/jbt.23604>
- Ileriturk, M., Kandemir, O., Akaras, N., Simsek, H., Genc, A., & Kandemir, F. M. (2023). Hesperidin has a protective effect on paclitaxel-induced testicular toxicity through regulating oxidative stress, apoptosis, inflammation and endoplasmic reticulum stress. *Reproductive toxicology*, 118, 108369. <https://doi.org/10.1016/j.reprotox.2023.108369>
- Kamel, R., El Morsy, E. M., Elsherbiny, M. E., & Nour-Eldin, M. (2022). Chrysin promotes angiogenesis in rat hindlimb ischemia: Impact on PI3K/Akt/mTOR signaling pathway and autophagy. *Drug development research*, 83(5), 1226-1237. <https://doi.org/10.1002/ddr.21954>
- Kandemir, F. M., Kucukler, S., Eldutar, E., Caglayan, C., & Gülçin, İ. (2017). Chrysin Protects Rat Kidney from Paracetamol-Induced Oxidative Stress, Inflammation, Apoptosis, and Autophagy: A Multi-Biomarker Approach. *Scientia pharmaceutica*, 85(1), 4. <https://doi.org/10.3390/scipharm85010004>
- Kandemir, F. M., Ileriturk, M., & Gur, C. (2022). Rutin protects rat liver and kidney from sodium valproate-induced damage by attenuating oxidative stress, ER stress, inflammation, apoptosis and autophagy. *Molecular biology reports*, 49(7), 6063-6074. <https://doi.org/10.1007/s11033-022-07395-0>
- Kankılıç, N. A., Küçükler, S., Gür, C., Akarsu, S. A., Akaras, N., Şimşek, H., et al. (2024). Naringin protects against paclitaxel-induced toxicity in rat testicular tissues by regulating genes in pro-inflammatory cytokines, oxidative stress, apoptosis, and JNK/MAPK signaling pathways. *Journal of biochemical and molecular toxicology*, 38(7), e23751. <https://doi.org/10.1002/jbt.23751>
- Kuzu, M. A., Köksoy, C., Kale, I. T., Tanık, A., Terzi, C., & Elhan, A. H. (1998). Reperfusion injury delays healing of intestinal anastomosis in a rat. *The American journal of surgery*, 176(4), 348-351. [https://doi.org/10.1016/s0002-9610\(98\)00198-6](https://doi.org/10.1016/s0002-9610(98)00198-6)
- Li, Y., Xu, B., Xu, M., Chen, D., Xiong, Y., Lian, M., ... & Lin, Y. (2017). 6-Gingerol protects intestinal barrier from ischemia/reperfusion-induced damage via inhibition of p38 MAPK to NF-κB signalling. *Pharmacological research*, 119, 137-148. <https://doi.org/10.1016/j.phrs.2017.01.026>
- Livak, K.J., and Schmittgen, T.D. (2001). Analysis of relative gene expression data using real-time quantitative PCR and the 2(-Delta Delta C(T)) Method. *Methods*, 25(4), 402–408. <https://doi.org/10.1006/meth.2001.1262>
- Lowry, O. H., Rosebrough, N. J., Farr, A. L., & Randall, R. J. (1951). Protein measurement with the Folin phenol reagent. *The Journal of biological chemistry*, 193(1), 265–275.
- Megison, S. M., Horton, J. W., Chao, H. E., & Walker, P. B. (1990). A new model for intestinal ischemia in the rat. *Journal of surgical research*, 49(2), 168-173. [https://doi.org/10.1016/0022-4804\(90\)90257-3](https://doi.org/10.1016/0022-4804(90)90257-3)
- Osmanlioğlu, Ş., Arslan, M., Dağ, R. O., Yiğman, Z., Ceyhan, M. Ş., Er, F., & Kavutçu, M. (2023). Artemisinin reduces acute ovarian ischemia-reperfusion injury in rats. *Reproductive toxicology*, 119, 108417. <https://doi.org/10.1016/j.reprotox.2023.108417>
- Park, P. O., & Haglund, U. L. F. (1992). Regeneration of small

- bowel mucosa after intestinal ischemia. *Critical care medicine*, 20(1), 135-139. <https://doi.org/10.1097/00003246-199201000-00026>
- Placer, Z. A., Cushman, L. L., & Johnson, B. C. (1966). Estimation of product of lipid peroxidation (malonyl dialdehyde) in biochemical systems. *Analytical biochemistry*, 16(2), 359-364. [https://doi.org/10.1016/0003-2697\(66\)90167-9](https://doi.org/10.1016/0003-2697(66)90167-9)
- Rana S. V. S. (2020). Endoplasmic Reticulum Stress Induced by Toxic Elements-a Review of Recent Developments. *Biological trace element research*, 196(1), 10-19. <https://doi.org/10.1007/s12011-019-01903-3>
- Refaie, M. M., & El-Hussieny, M. (2018). Protective effect of pioglitazone on ovarian ischemia reperfusion injury of female rats via modulation of peroxisome proliferator activated receptor gamma and heme-oxygenase 1. *International immunopharmacology*, 62, 7-14. <https://doi.org/10.1016/j.intimp.2018.06.037>
- Sedlak, J., & Lindsay, R. H. (1968). Estimation of total, protein-bound, and nonprotein sulfhydryl groups in tissue with Ellman's reagent. *Analytical biochemistry*, 25(1), 192-205. [https://doi.org/10.1016/0003-2697\(68\)90092-4](https://doi.org/10.1016/0003-2697(68)90092-4)
- Semis, H. S., Kandemir, F. M., Kaynar, O., Dogan, T., & Arikan, S. M. (2021). The protective effects of hesperidin against paclitaxel-induced peripheral neuropathy in rats. *Life sciences*, 287, 120104. <https://doi.org/10.1016/j.lfs.2021.120104>
- Simsek, H., & Akaras, N. (2023). Acacetin ameliorates acetylsalicylic acid-induced gastric ulcer in rats by interfering with oxidative stress, inflammation, and apoptosis. *International journal of medical biochemistry*, 6(2). <https://doi.org/10.14744/ijmb.2023.07830>
- Şimşek, H., Akaras, N., Gür, C., Küçükler, S., & Kandemir, F. M. (2023a). Beneficial effects of Chrysin on Cadmium-induced nephrotoxicity in rats: Modulating the levels of Nrf2/HO-1, RAGE/NLRP3, and Caspase-3/Bax/Bcl-2 signaling pathways. *Gene*, 875, 147502. <https://doi.org/10.1016/j.gene.2023.147502>
- Şimşek, H., Küçükler, S., Gür, C., Akaras, N., & Kandemir, F. M. (2023b). Protective effects of sinapic acid against lead acetate-induced nephrotoxicity: a multi-biomarker approach. *Environmental science and pollution research*, 30(45), 101208-101222. <https://doi.org/10.1007/s11356-023-29410-y>
- Şimşek, H., Küçükler, S., Gür, C., İleritürk, M., Aygörmmez, S., & Kandemir, F. M. (2023c). Protective effects of zingerone against sodium arsenite-induced lung toxicity: A multi-biomarker approach. *Iranian journal of basic medical sciences*, 26(9), 1098. <https://doi.org/10.22038/IJBMS.2023.71905.15623>
- Talebi, M., Talebi, M., Farkhondeh, T., Kopustinskiene, D. M., Simal-Gandara, J., Bernatoniene, J., & Samarghandian, S. (2021). An updated review on the versatile role of chrysin in neurological diseases: Chemistry, pharmacology, and drug delivery approaches. *Biomedicine & pharmacotherapy*, 141, 111906. <https://doi.org/10.1016/j.biopha.2021.111906>
- Yakut, S., Atcalı, T., Çağlayan, C., Ulucan, A., Kandemir, F. M., Kara, A., & Anuk, T. (2024). Therapeutic Potential of Silymarin in Mitigating Paclitaxel-Induced Hepatotoxicity and Nephrotoxicity: Insights into Oxidative Stress, Inflammation, and Apoptosis in Rats. *Balkan medical journal*, 41(3), 193. <https://doi.org/10.4274/balkanmedj.galenos.2024.2024-1-60>
- Yesildag, K., Gur, C., İleritürk, M., & Kandemir, F. M. (2022). Evaluation of oxidative stress, inflammation, apoptosis, oxidative DNA damage and metalloproteinases in the lungs of rats treated with cadmium and carvacrol. *Molecular biology reports*, 1-11. <https://doi.org/10.1007/s11033-021-06948-z>
- Yıldız, M. O., Çelik, H., Çağlayan, C., Kandemir, F. M., Gür, C., Bayav, İ., ... & Kandemir, Ö. (2022). Neuromodulatory effects of hesperidin against sodium fluoride-induced neurotoxicity in rats: Involvement of neuroinflammation, endoplasmic reticulum stress, apoptosis and autophagy. *Neurotoxicology*, 90, 197-204. <https://doi.org/10.1016/j.neuro.2022.04.002>
- Zhou, H., Wang, S., Hu, S., Chen, Y., & Ren, J. (2018). ER-mitochondria microdomains in cardiac ischemia-reperfusion injury: A fresh perspective. *Frontiers in physiology*, 9, 755. <https://doi.org/10.3389/fphys.2018.00755>
- Zou, L., Attuwaybi, B., & Kone, B. C. (2003). Effects of NF-kappa B inhibition on mesenteric ischemia-reperfusion injury. *American journal of physiology. Gastrointestinal and liver physiology*, 284(4), G713-G721. <https://doi.org/10.1152/ajpgi.00431.2002>